Copy from the Proc. 11th Int. Modal Analysis Conf., Kissimmee, February 1-4, 1993, Vol. II. 1366-1374.p.

VIBRO-ACOUSTIC MODAL ANALYSIS OF A DOUBLE WALL STRUCTURE

P. Sas
Professor

KU Leuven
Mech. Eng. Dept.
B-3001 Leuven
Celestijnenlaan 300B
Belgium

F. Augusztinovicz
Visiting researcher at KUL

Inst. for Transport Sciences
Acoustics Dept.
H-1119 Budapest
Thán K. u. 3-7.
Hungary

J. Van de Peer
Research Assistent

KU Leuven
Mech. Eng. Dept.
B-3001 Leuven
Celestijnenlaan 300B
Belgium

ABSTRACT

The aim of the paper is to investigate the vibroacoustic behaviour of a simple, finite, double wall structure model: a shallow, rectangular acoustical cavity composed of two parallel plates clamped to a rigid steel framework. This structure is analyzed by means of analytical, numerical and experimental methods. The analytical treatment of the testing object is based on an orthogonal modal expansion of the response of the coupled acoustic-structural system. The numerical calculations use a coupled structural FE - acoustical BE method, carried out in three consecutive steps. The aim of the experiments is to verify the results of the calculations, with special emphasis on the visualization of the sound field in the coupling cavity between the plates of the double wall model. The calculated and measured results are discussed in details, they are compared in tables and in figures and conclusions are drawn with special regard to application of the applied numerical technique for transmission loss predictions and for active noise control.

NOMENCLATURE

$[A_{am}]$	coupling submatrix
$[B_{am}]$	coupling submatrix
c	sound speed in air
$[\hat{C}]$	modal coupling matrix
d	distance of plates
D	bending stiffness of the plate
f	frequency; force
$\underline{F}$	column vector of generalized external forces
E_A	column vector of external acoustic forces
$\underline{F}_S$	column vector of external structural forces
$\underline{\hat{F}}_S$	column vector of modal forces
H(k)	boundary element system matrix, see Eq. (10)
k	stiffness
$[K_S]$	structural stiffness matrix
$[\hat{K}_S]$	modal stiffness matrix
m	mass per unit area
$[M_S]$	structural mass matrix
$[\hat{M}_S]$	modal mass matrix
$\underline{Q}$	column vector of generalized source strengths
p	sound pressure
$\underline{P}$	column vector of acoustic potentials
$\vec{r}$	position vector
t	time
$\underline{U}$	nodal displacement vector
w	plate displacement
W_m	modal coordinate of coupled structural mode
$\underline{W}$	column vector of structural mode shapes
x_i	participation factor
$\underline{x}$	column vector of participation factors
ρ_0	mean density of air
$\underline{\phi}$	column vector of acoustical mode shapes
Φ	velocity potential
Φ_a	modal coordinate of coupled acoustic mode in terms of velocity potential
$\underline{\Psi}_i$	uncoupled structural modeshape
$[\Psi]$	matrix of uncoupled structural modeshapes
ω	angular frequency
$[\Omega_a]$	general diagonal submatrix with acoustic eigenvalues
$[\Omega_m]$	general diagonal submatrix with structural eigenvalues

1. INTRODUCTION

Double wall structures are often used in noise control and in other fields of acoustical engineering, when relatively high Transmission Loss has to be achieved by using light-weight structures. Unfortunately, due to various fluid-structure interaction effects the performance of a double wall is not just the sum of those of the two single layers, and for low frequencies it can even fall short of one of the walls alone. The application of active noise control methods can offer a viable solution in these cases [11]. However, the realization of an effective ANC system requires the thorough understanding of the vibro-acoustical coupling between the mechanical and acoustical elements of a double wall, whether vibration or acoustic secondary control sources are utilized.

The analysis of double wall structures goes back to the classical results of Beranek and Work [1] and London [2]. Later Cremer and Heckl [3] and Fahy [4] gave a detailed description of the physical behaviour of double-wall structures. These models were extended by taking into account also the effect of cavity absorption [5,6]. Recently, an analytical method was presented to handle various layered systems consisting of porous materials [7]. All of these models and methods refer to plane, infinite plates; the edge effects caused by the finite dimensions of the samples are not considered.

The aim of this paper is to study the mechanism of vibro-acoustical coupling in details in light-weight, double wall structures of finite dimensions for low frequencies, i.e., below the mass controlled region. We have performed analytical, numerical and experimental modal investigations on a simple double wall structure; all of these approaches are shortly discussed, the obtained results presented and compared. Finally, keeping in mind the needs of the ANC application, the experimental modal analysis of the normal modes is extended to include the forced response of the system.

2. ANALYTICAL INVESTIGATIONS

2.1. "Classical" analytical models of double wall structures in the low frequency range

The usual analytical models of an infinite double wall structure consist of two infinite parallel, uniform plates separated by a cavity of finite depth, filled with air, see Fig.1a. The simplest way of treating this system is to assume that the plates are non-flexible [4]. By neglecting the stiffness of the plates one can then show that the Transmission Loss of the structure drops to a minimum at the frequency

$$f_0 = \frac{1}{2\pi}\left[\frac{\rho_0 c^2}{d}\left(\frac{m_1+m_2}{m_1 m_2}\right)\right]^{1/2} \qquad (1)$$

The air gap between the two plates acts as though it was a set of springs, distributed uniformly over the plates. Therefore, f_0 is often referred to as the *mass-air-mass* resonance frequency of the structure.

From a modal point of view, this system corresponds to a simple two dof system, see Fig.1b., thus having two natural frequencies:

$$f_{01} = 0 \qquad (2a)$$

which corresponds to a rigid body mode and

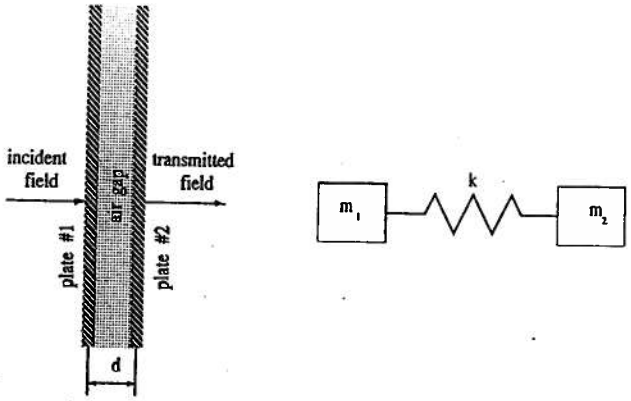

Fig.1. Physical models of an infinite double wall structure

$$f_{02} = \frac{1}{2\pi}\left[k\left(\frac{m_1+m_2}{m_1 m_2}\right)\right]^{1/2} \qquad (2b)$$

For our acoustic system the zero frequency mode is irrelevant, therefore the infinite double wall structure is characterized by one single mode, the frequency of which is given by Eq.(1). Note that Eq.(1). is identical to Eq.(6.22) in [2] if the plates are alike.

A more detailed physical insight can be gained if the plates are assumed to be flexible. The theoretical analysis as performed e.g. in [3] shows that the governing coupled equation has two sets of solutions, characterized by two different wavenumbers and associated deflections. The coupled system supports flexural waves with usually lower wavenumbers than the same plates do *in vacuo* and at a certain frequency, which can be shown to be identical to those given by Eq.(1), the lower wavenumber vanishes. The associated sets of solutions are characterized by in-phase and 180° out of phase plate deflections, respectively. Nevertheless, this more realistic model still has only one single meaningful natural mode of vibration, at least as long as the depth of the cavity is smaller than the half wavelength in air.

2.2. Analytical modelling of fluid-structure interaction in a finite double-wall partition

Let the next analytical model consist of two plane, parallel, flexible plates of the same size, clamped airtight to a rigid framework and baffled in an infinite rigid wall. The length and width of the plates are assumed to be in the same order of magnitude as the wavelength in air for the frequency range of interest while the distance of the plates, i.e., the cavity depth, is still thought to be negligible. Due to the fact that this system is bounded in all directions, one can in principle anticipate an infinite number of natural modes.

The chosen analytical treatment is based on the modal expansion method [8]. This theory is summarized and its extension for a double wall structure is presented in [11], therefore the most important steps of the derivation are repeated here only.

The sound field in the cavity is governed by the inhomogeneous wave equation:

$$\nabla^2 p(\bar{r},t) - \frac{1}{c^2}\frac{\partial^2 p(\bar{r},t)}{\partial t^2} = -\rho_0 \frac{\partial q(\bar{r},t)}{\partial t} \qquad (3)$$

One can assume that the solution takes the form of an orthogonal modal expansion:

$$p(\bar{r},\omega,t) = \sum_{a=0}^{\infty} \Phi_a(\bar{r})\, P_a(\omega,t) \qquad (4)$$

Here Φ_a is the spatial characteristic function of the ath mode of the cavity with rigid walls and P_a is the time- and frequency-dependant modal amplitude, representing the relative contribution of the ath uncoupled acoustic mode to the coupled solution. Φ_a is *a priori* known while the P_a values are to be determined for the relevant system.

The vibrations of the plates (further referred to as structure) are governed by the following equation:

$$D\,\nabla^4 w(\bar{r}_s) + m(\bar{r}_s)\,\frac{\partial^2 w(\bar{r}_s)}{\partial t^2} = f(\bar{r}_s) \qquad (5)$$

Again, the structural motion is expressed as a weighted sum of modes of the uncoupled subsystem, i.e., the *in vacuo* modes of the structure:

$$w(\bar{r}_s,\omega,t) = \sum_{m=1}^{\infty} \Psi_m(\bar{r}_s)\, W_m(\omega,t) \qquad (6)$$

where, as opposed to Eq.(4), the plate modes are summed on the surface of the cavity.

The derivation of the coupled modal equations yields two infinite sets of differential equations with unknowns of the modal amplitudes of the sound pressure and plate displacement series expansion. Assuming that the number of the considered acoustical modes is constrained to n and that of the structural modes to m, these differential equations can be converted into a practical matrix form

$$\left[\begin{array}{c|c} \underline{\underline{\Omega_a}} & \underline{\underline{A_{am}}} \\ \hline \underline{\underline{B_{am}}} & \underline{\underline{\Omega_m}} \end{array}\right] \left[\begin{array}{c} \underline{\phi} \\ \underline{W} \end{array}\right] = \left[\begin{array}{c} \underline{Q} \\ \underline{F} \end{array}\right] \qquad (7)$$

where $\underline{\underline{\Omega_a}}$ and $\underline{\underline{\Omega_m}}$ are diagonal matrices with the modal frequencies of the uncoupled acoustical and structural subsystems and $\underline{\underline{A_{am}}}$ and $\underline{\underline{B_{am}}}$ are coupling submatrices. $\underline{\phi}$ and $\underline{W}$ are mode shape vectors, representing the amplitude of the acoustical and structural modes contributing to the overall response of the coupled, vibroacoustic system, and $\underline{Q}$ and $\underline{F}$ represent the possible inputs thereof. The resulting matrix contains terms of both first and second power of the eigenvalue, and therefore poses a non-standard eigenvalue problem. This difficulty can, nevertheless, be easily overcome by using appropriate matrix transformation methods [9] and the eigenvalues can be calculated.

Eq. (7) represents the general mathematical formulation of the fluid-structure interaction problem. To apply this formulation for our transmission calculations, the theory has to be adapted for a double wall structure and an appropriate excitation field has to be defined. It was assumed that the excitation field is realized by a loudspeaker source positioned in a relatively small sound-proof enclosure, embedding the testing structure on its top, see Fig.2. Thus, the system to be analyzed is composed of two cavities and two plates and coupling takes place between each pair of adjacent elements such as test enclosure (cavity #2) - bottom plate (plate #2), bottom plate - air gap (cavity #1) and air gap - upper plate (plate #1). Consequently, Eq. (7) can be decomposed into four different fields and we obtain

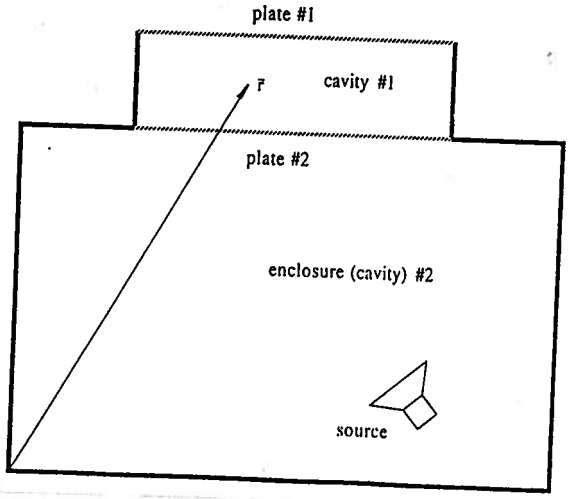

Fig.2. Physical model of a finite double wall structure

$$\left[\begin{array}{cccc} \underline{\underline{\Omega_{a1}}} & \underline{\underline{0}} & \underline{\underline{A_{11}}} & \underline{\underline{A_{12}}} \\ \underline{\underline{0}} & \underline{\underline{\Omega_{a2}}} & \underline{\underline{0}} & \underline{\underline{A_{21}}} \\ \underline{\underline{B_{11}}} & \underline{\underline{0}} & \underline{\underline{\Omega_{m1}}} & \underline{\underline{0}} \\ \underline{\underline{B_{21}}} & \underline{\underline{B_{22}}} & \underline{\underline{0}} & \underline{\underline{\Omega_{m2}}} \end{array}\right] \left[\begin{array}{c} \underline{\phi_1} \\ \underline{\phi_2} \\ \underline{W_1} \\ \underline{W_2} \end{array}\right] = \left[\begin{array}{c} \underline{Q_1} \\ \underline{Q_2} \\ \underline{F_1} \\ \underline{F_2} \end{array}\right] \qquad (8)$$

The solution of Eq. (8) and the subsequent calculations are perfectly analogous to those of Eq. (7) with the necessary extensions.

The physical interpretation of this coupling equation is that due to the presence of the cavity the response of the sorrounding structure will be determined by combination of a number of its uncoupled modes rather than by a single one and *vica versa*. This mechanism of the coupling of n acoustic and m structural modes results in $n+m$ common eigenvalues, associated with their eigenvectors, and eventually yields a vibration and sound field in the coupled system which can be significantly different from those of the uncoupled constituting elements.

2.3. Results of calculations

Eq.(8) was used to calculate the natural frequencies and mode shapes of the coupled system, based on numerically calculated *in vacuo* eigenfrequencies of the plates as discussed below. As noted by other authors [e.g. 9], the coupling is selective: only a few combination of modes result in finite values. Therefore, the coupling submatrices are relatively sparse (which, in turn, can be exploited to perform the calculations more fast and economically) and the coupling between structural and cavity modes results in four groups of coupled eigenfrequencies. Three of these groups together with the uncoupled structural and acoustical mode frequencies and mode shapes are summarized in Table 1. below. One can see that the calculated coupled frequencies hardly differ from the uncoupled structural modal frequencies. On the other side, significant deviations can be found between the uncoupled and coupled acoustical mode frequencies.

As can be expected, the calculated coupled mode shapes are combinations of the constituting uncoupled modes, but in several cases dominated by one of them. Some typical coupled structural modes are depicted in Figs. 3a. to 3d. Comparing them to their uncoupled counterpart, one can conclude that the presence of the cavity only slightly modifies the behaviour of the structural response.

Table 1
Calculation of the coupled resonance frequencies, based on *in vacuo* structural and rigid wall acoustical modes

Numerically calculated uncoupled structural resonance frequencies		Analytically calculated resonance frequencies of the coupled system, by considering two uncoupled acoustic modes			
		Freq	Freq	Freq	Freq
Freq [Hz]	Mode sh	0 Hz (0,0,0) 301.8 Hz (2,0,0)	149.1 Hz (1,0,0) 447.4 Hz (3,0,0)	233 Hz (0,1,0) 378 Hz (2,1,0)	279.8 Hz (1,1,0) 504.3 Hz (3,1,0)
16.6	1,1	0			
24.8	2,1		22.0		
38.9	3,1	35.7			
41.1	1,2			38.9	
48.5	2,2				46.8
58.7	4,1		57.0		
61.3	3,2			60.0	
78.2	1,3	68.7			
79.6	4,2				78.6
83.9	5,1	82			
85.1	2,3		83.9		
96.9	3,3	94.4			
103.4	5,2			102.9	
113.5	4,3		112.3		
114.5	6,1		113.8		
127.6	1,4			126.3	
132.6	6,2				132.1
134.2	5,3	134.3			
136.3	2,4				135.5
145.3	3,4			144.7	
150.3	7,1	150.6			
161.1	4,4				160.7
163.9	6,3		162.8		
167.5	7,2			167.0	
182.2	5,4			182.0	
189.5	8,1		191.3		
191.2	1,5	191.1			
195.4	7,3	195.5			
197.1	2,5		200.1		
205.5	8,2				204.9
206.4	6,4				206.3
208.4	3,5	208.3			
221.1	4,5		221.3		
234.7	8,3		234.8		
237.2	9,1	237			
239.1	7,4			238.6	
241.3	5,5	241.3			
252.3	9,2			247.3	
		101.7	171.6	255.5	293.9
		317.5	456.7	388.7	511.7

Perhaps the best examples to visualize this behaviour of the coupled cavity are those gained from coupling with the (0,0,0)/(2,0,0) cavity modes. A number of coupled cavity modes in this group show mode shapes similar to those depicted in Fig. 4a. That is, standing waves characterized by small or negligeable spatial variation can exist in the cavity. Other acoustic modes show the effects of higher modes as shown in Fig. 4b. to 4d.

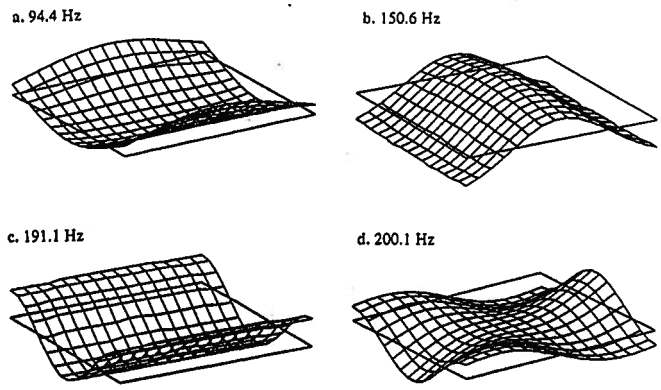

Fig.3. Calculated structural mode shapes of the coupled system

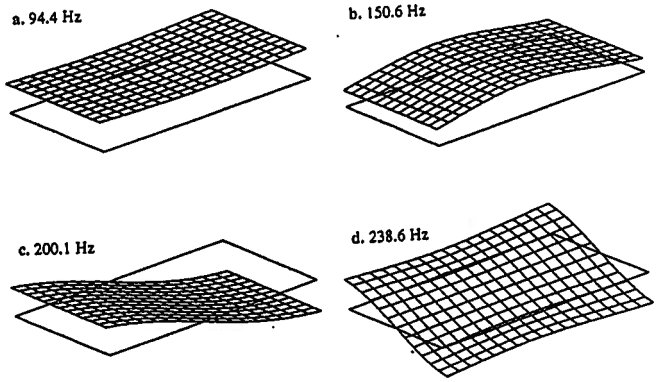

Fig.4. Calculated acoustical mode shapes of the coupled system

3. EXPERIMENTAL INVESTIGATIONS

3.1. Measuring conditions

The aim of the measurements was to verify the results of the theoretical calculations by making detailed measurements on the enclosing plates and within the cavity. Special attention was paid to visualize the sound field within the cavity, the coupling element between the two walls of the testing object, by making use of a fixed microphone array composed of small microphones.

Our simple structure chosen for the validation measurements consisted of two plane, parallel aluminium plates of thickness 1.5 mm, clamped to a 10 mm thick, 150 mm high rectangular, welded steel framework. The free dimensions of the plates are 1140 x 730 mm. This testing object was instrumented by an array of 48 small microphones in the medium plane of the cavity as well as 36 to 48 accelerometers on both plates. The microphone spacing of the 8 x 6 mesh was 120 x 127 mm, aimed at mapping the sound pressure in the whole cavity as far as possible. The accelerometers were placed in a 6 x 6 mesh with 60 mm spacing in the central part of the plates. Both the microphones and the accelerometers were manufactured by PCB Piezotronics, Inc. (Types Structcel and Acousticel, respectively). Following these preparatory work the instrumented testing object was placed in the opening of a test box designed specifically for this purpose. All the measurements and the subsequent modal analyses were

carried out by means of an LMS CADA-X measurement/analysis system, based on a 16-channel DIFA Scadas data acquisition unit and a Hewlett Packard 9000 Series 385 workstation. More details of the measurement system can be found in [10] and [11].

The modal analyses were based on FRF measurements with reference to different control microphones placed in the test box. The measurements on plate#1 were performed with closed cavity and also with removed plate#2; this enables one to analyse the effect of the cavity on the structural response of one of the plates.

3.2. Measurement results

The sum of measured FRFs on the bottom plate with and without cavity, referenced to the sound pressure in the enclosure, is compared to the sum of sound pressure FRFs measured within and above the cavity (with the same reference), as well as to the measured intensity in Fig. 5. The modal frequencies are also summarized in Table 2. It is seen that the most important resonance peaks in the cavity and on the plates are common in frequency but their relative

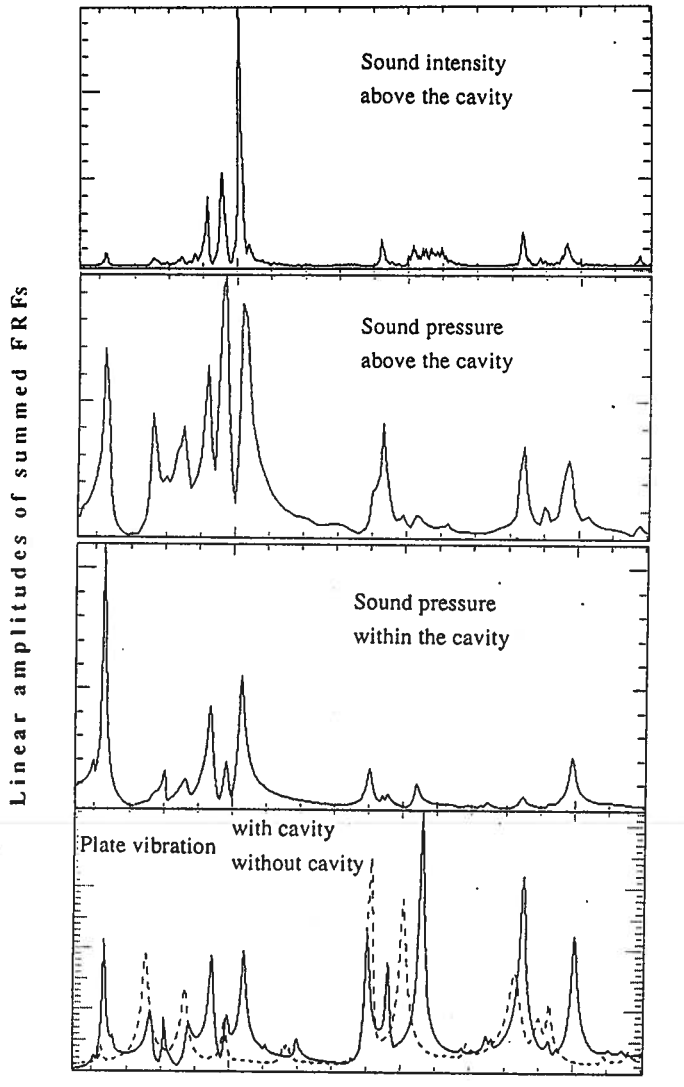

Fig.5. Comparison of averaged FRFs

Table 2 Comparison of experimentally determined resonance frequencies and mode shapes

Structural modes				Acoustic modes	
Uncoupled		Coupled		Coupled	
Freq [Hz]	Mode shape	Freq [Hz]	Mode shape	Freq [Hz]	Mode shape
43.8	3,1				
62.7	4,1	63.4		62.8	0,0,0
		65.8			
75.4	1,3	76.9	1,3		
		80.9		79.9	0,0,0
86.8	5,1	87.8		86.7	0,0,0
		94.8		93.5	0,0,0
		98.9		98.2	0,0,0
98.5	3,3	104.0	3,3	102.7	0,0,0
116.5	4,3	119.9		118.0	
121.5				121.0	
123.2					
134.4	6,2	136.3			
		140.2		140.0	
140.9	5,3	146.5	5,3	144.8	
150.6	7,1	155.8	7,1	153.7	
163.9	4,4	167.9	4,4	164.6	
169.4	7,2	175.3	7,2	174.4	
182.8	1,5	185.3		184.7	
190.0	8,1	193.2			
		195.6			
193.0	2,5	200.3		199.3	1,0,0
208.5		211.9			
211.4	3,5	213.8			
216.0	6,4	221.6	6,4	220.6	
223.8	4,5	228.4	4,5	226.6	
233.8	9,1	238.6	9,1	237.5	0,1,0
251.0	9,2	249.1		249.5	

amplitude is highly different. After closing the cavity, i.e., in the coupled system, the resonances of plate#1 are generally shifted towards higher frequencies but some new frequencies appear as well.

When considering the structural mode shapes and comparing the coupled and uncoupled mode shapes found for plate#1, one can in general say that the coupled mode shapes stem from a combination of the uncoupled ones. Again, a number of coupled modes are strongly influenced by one single uncoupled mode. (In these cases the mode shape numbers of the identified dominant uncoupled mode are also given in the second column of Table 2). Fig.6. shows some of the typical structural mode shape pairs obtained for plate#1. Note that the measured modal frequencies and the mode shapes of plate#2 are very similar to those of plate#1, therefore they are not shown separately. It is worth to mention, nevertheless, that for almost all mode frequencies the plates respond with the same mode shape but out-of-phase.

Fig.7. depicts some typical mode shapes of the cavity, encountered at various important resonance frequencies in the cavity. Mode shapes found in the low frequency range (appr. below 110 Hz) are more or less similar to those shown in Fig.7a., but with increasing frequency the modes are more and more combined. Fig.7c. shows the clear effect of the (1,0,0) mode and at 237 Hz a relatively pure (0,1,0) mode can be found (Fig.7d.).

Although the comparison of results from different approaches is delayed to paragraph 5., it is instructive to

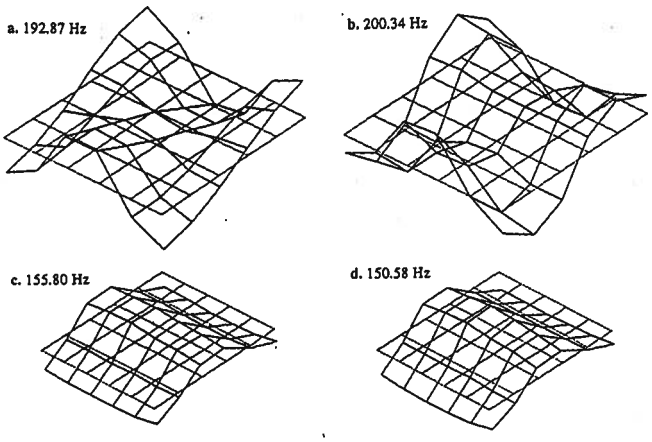

Fig.6. Comparison of measured mode shapes of the bottom plate without cavity (left side) and with cavity (right side)

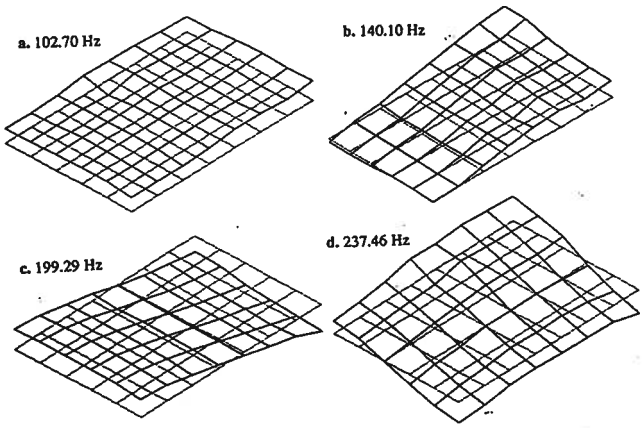

Fig.7. Measured acoustic mode shapes of the cavity

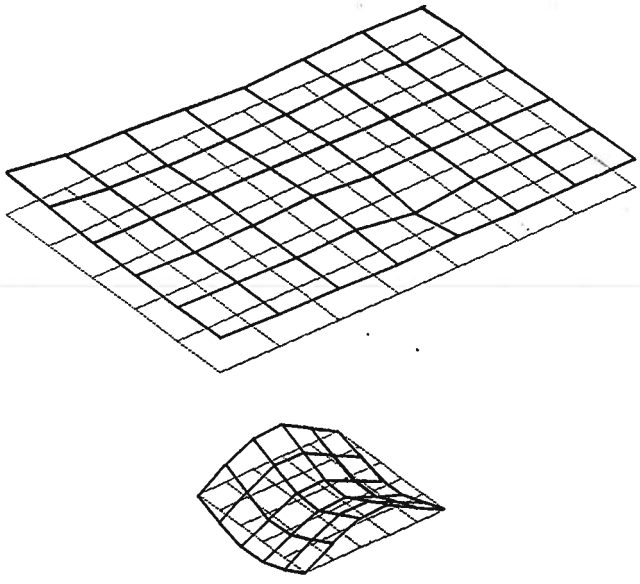

Fig.8. Comparison of structural and acoustical mode shapes in the same geometrical scale for a 94 Hz mode

compare here the mode shapes in the cavity and for the coupling plate#1 for a common important resonance frequency, such as shown in Fig.8. In spite of the significant deviation of the mode shapes, the performed acoustic insertion loss measurements revealed high transmissions at these resonance frequencies, suggesting that in spite of the highly different mode shapes the degree of coupling between the fluid and the structure is high.

4. NUMERICAL CALCULATIONS

4.1 Applied method

In order to numerically represent the above described test situation, a coupled FEM-BEM formulation (provided in the program SYSNOISE) was chosen, in which the structure was modelled with finite elements, and the fluid was modelled with boundary elements, both combined in one computational scheme to solve the total vibro-acoustic problem. Both the structural FE and acoustic BE part are modelled by means of a variational approach.

The numerical analysis is based on two matrix equations, referring to the structural and the acoustical subsystem, respectively:

$$\left([K_S]-\omega^2[M_S]\right)\underline{U}+[C]^T\underline{P}=\underline{F}_S \qquad (9)$$

$$\frac{1}{\rho_F\omega^2}[H(k)]\underline{P}+[C]\underline{U}=\underline{F}_A \qquad (10)$$

Writing both equations together in one single matrix one obtains:

$$\begin{bmatrix} K_S-\omega^2M_S & C^T \\ C & \dfrac{H(k)}{\rho_0\omega^2} \end{bmatrix}\begin{bmatrix}\underline{U}\\ \underline{P}\end{bmatrix}=\begin{bmatrix}\underline{F}_S\\ \underline{F}_A\end{bmatrix} \qquad (11)$$

In order to reduce the number of degrees of freedom in the system and hence to reduce computation time, it is possible to use structural modal coordinates instead of physical ones. The nodal displacement vector is then projected on a structural modal base and represented as

$$\underline{U}=\sum_{i=1}^{n}\underline{\Psi}_i.x_i \qquad (12)$$

Thus $\underline{U}$ can be written as a sum of n included (uncoupled) structural mode shapes $\underline{\Psi}_i$ multiplied by a (complex) participation factor x_i.

With the formalism of Eq. (12), Eq. (11) becomes:

$$\begin{bmatrix} [\hat{K}]_S-\omega^2[\hat{M}]_S & [\hat{C}] \\ [\hat{C}]^T & \dfrac{[H(k)]}{\rho_0\omega^2} \end{bmatrix}\begin{bmatrix}\underline{x}_i\\ \underline{P}\end{bmatrix}=\begin{bmatrix}\underline{\hat{F}}_S\\ \underline{F}_A\end{bmatrix} \qquad (13)$$

After having solved this equation for a certain frequency, the structural displacements and the acoustic potentials are known. From these potentials, the acoustic pressure and particle velocity in any point in the fluid can be calculated.

An important advantage of the use of this modal base is just the possibility to monitor the participation factors, in order to gain a better understanding of the modal coupling between the structure and the fluid. Structural modes that couple well with the fluid at a certain frequency will show high participation factors. Accordingly, the deformation pattern of the structure will be determined by the mode shapes of those well-coupling modes.

4.2. Calculations

First a set of 80 uncoupled structural modes was calculated by means of the structural FE package SYSTUS. The resulting modal frequencies and displacement patterns are summarised in Table 3. The notations L and W in the table indicate the number of displacement maxima in the longitudinal and transversal direction of the plates, respectively.

As a second step the coupled responses were calculated over the frequency band 50 to 220 Hz with a frequency step of 0.5 Hz. As a result, the participation factors of the structural modes in the coupled responses, the new deformation patterns and the pressure maps between the plates were determined. Note that in the course of this numerical simulation only forced responses in a certain frequency range have been calculated. (For the time being, mode extraction by means of boundary element formulation is not possible.) Although no coupled modes can directly be found in this way, we can say with high certainty that the modes will occur at the peaks in a frequency response curve, since no damping was included into the model. The maximum error in frequency is 0.5 Hz.

Upper plate

Mode	Freq. [Hz]	Modeshape L	Modeshape W
1	16.606	1	1
3	24.783	2	1
5	38.809	3	1
7	41.136	1	2
9	48.457	2	2
11	58.344	4	1
13	61.102	3	2
15	78.181	1	3
17	79.208	4	2
19	83.174	5	1
21	84.968	2	3
23	96.596	3	3
25	102.73	5	2
27	113.07	6	1
28	113.46	4	3
31	127.60	1	4
33	131.60	6	2
35	133.96	2	4
37	135.28	5	3
39	144.75	3	4
41	148.46	7	1
43	160.26	4	4
45	162.58	6	3
47	165.82	7	2
49	180.73	5	4
51	188.94	8	1
52	189.46	1	5
55	195.24	7	3
56	195.41	2	5
59	205.26	8	2
60	205.50	3	5
62	206.42	6	4
65	219.95	4	5
67	233.30	8	3
68	234.70	9	1
70	237.22	7	4
72	239.07	5	5
75	250.22	9	2
77	263.08	6	5
78	263.95	1	6

Lower plate

Mode	Freq. [Hz]	Modeshape L	Modeshape W
2	16.610	1	1
4	24.813	2	1
6	38.930	3	1
8	41.147	1	2
10	48.511	2	2
12	58.680	4	1
14	61.263	3	2
16	78.206	1	3
18	79.559	4	2
20	83.895	5	1
22	85.088	2	3
24	96.875	3	3
26	103.40	5	2
29	113.89	4	3
30	114.46	6	1
32	127.65	1	4
34	132.61	6	2
36	134.15	2	4
38	136.34	5	3
40	145.26	3	4
42	150.27	7	1
44	161.12	4	4
46	163.94	6	3
48	167.50	7	2
50	182.15	5	4
53	189.53	1	5
54	191.18	8	1
57	195.70	2	5
58	197.15	7	3
61	206.07	3	5
63	207.28	8	2
64	208.44	6	4
66	221.13	4	5
69	235.14	8	3
71	237.50	9	1
73	239.48	7	4
74	241.31	5	5
76	252.31	9	2
79	264.01	1	6
80	265.26	6	5

4.3. Results of calculation

Fig.9. shows the sum of the frequency response functions (pressure over source input velocity) of the 48 equally spaced points in the middle plane between the two plates. This figure clearly shows that the cavity response is not only determined by the geometry of the cavity. The high peaks indicate that the two plates highly influence the amplitude of the response. As the frequency increases, the pressure pattern slightly shifts from a (0,0,0) behaviour over a (1,0,0) even towards a (2,0,0) behaviour. This trend can be illustrated in Fig.10., in which the pressure amplitude in the medium plane of the cavity is shown for frequencies of 79.5, 159 and 203.5 Hz, respectively. Note that the influence of the (0,1,0) mode on the pressure pattern was not found, due to the symmetric excitation in the y-direction, originating from the experimental configuration. The fact that the source is positioned at the left side in the box is well visible in the remarkably higher forced amplitudes at the left side of the cross section.

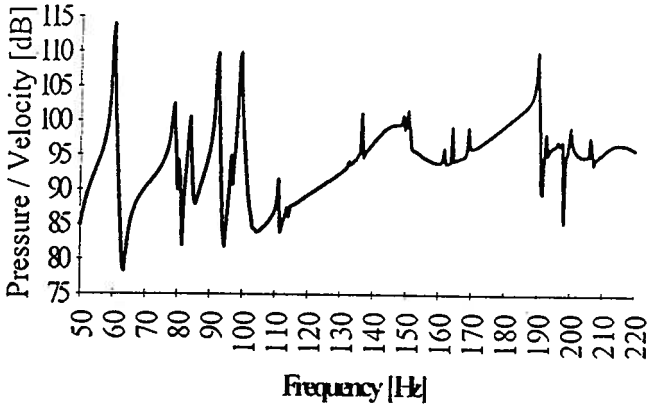

Fig.9. Averaged FRF, numerically calculated for the medium plane of the cavity

For the structural part, a detailed investigation of the deformation patterns at the same peaks of the frequency response function was performed. As already mentioned, the coupled displacement of the structure can be represented as a modal superposition of the uncoupled structural modes $\underline{\Psi}_i$, with the participation factors x_i as weighting factors. This property is demonstrated for a peak at 90 Hz in Fig.12. The deformation of the plates is shown together with a bar graph of the amplitudes of the participation factors of the uncoupled modes. (The plates are shown at a larger separation for reasons of clarity.) It is clear that the deformation pattern is dominated by a (1,3) + (5,1) + (3,3) behaviour. Due to the presence of the fluid, the displacements of the structure at a certain frequency are affected by different uncoupled modes, with original frequencies nearby the coupled frequency. Table 4 summarises the participation factors of the uncoupled modes for the different peaks of the above mentioned frequency response function. The less important modes are put between parentheses. It is striking that the participating uncoupled mode shapes mostly have an odd number of maxima in the transversal direction. Modes with an even number of maxima in that direction cannot be excited in the symmetric source configuration. The same information is depicted in Fig.12: the participation factors are shown in function of the uncoupled modes along the x-axis for the selected frequencies at the peaks along the y-axis.

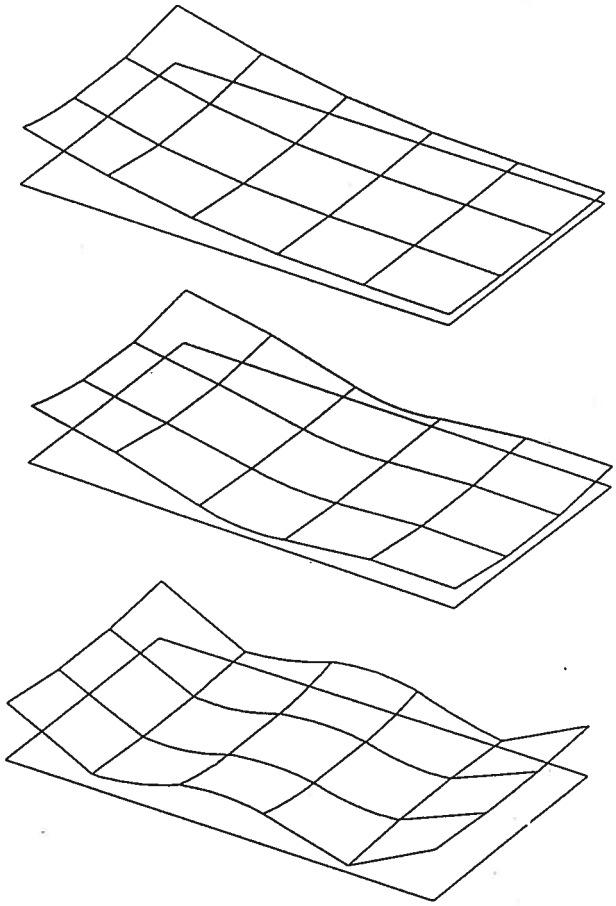

Fig.10. Amplitude of forced pressures, calculated for various frequencies

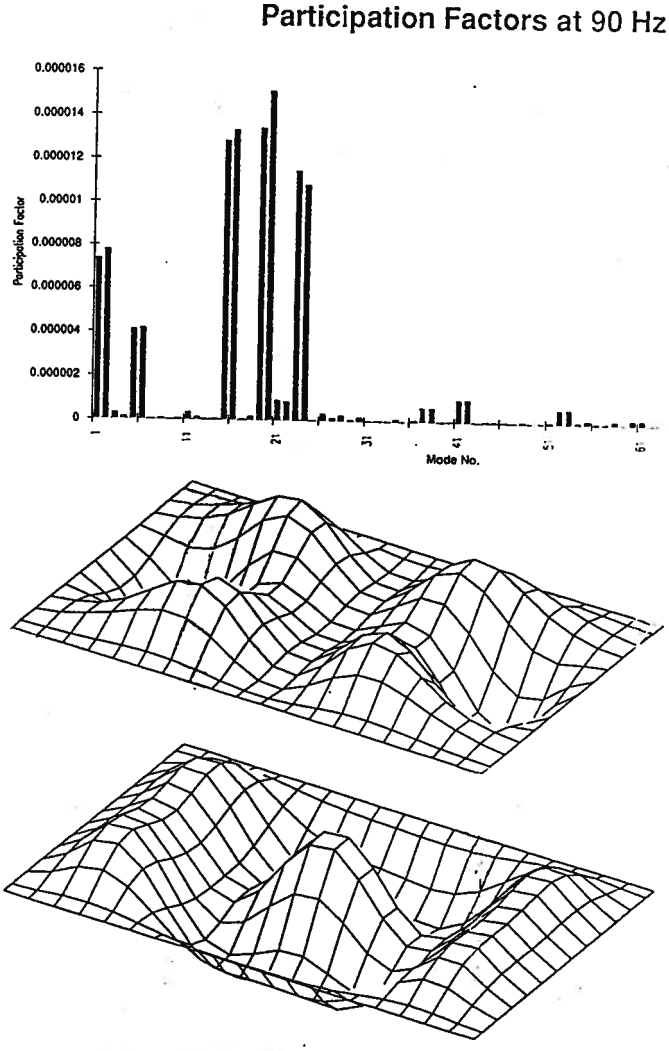

Fig.11. Forced displacement and participation factors calculated for the 90 Hz mode

Table 4. Coupled structural behaviour at selected frequencies

Freq. [Hz]	Main structural character
58.5	1,1 + 3,1 + 1,3 + (5,1)
79.5	1,3 + 5,1
82	2,3
90	1,3 + 5,1 + 3,3 + (1,1) + (3,1)
95.5	3,3
97	3,3 + (1,1) + (3,1) + (1,3) + (5,1)
110	6,1 + 4,3
135	5,3 (lower plate)
147	7,1
149	7,1 (lower plate)
159	4,4 + 6,3 + little (even,odd)
162	6,3 (lower plate)
165	6,3 + 7,2 + little (even,odd)
166	7,2 + (6,3) + little (even,odd)
188.5	1,5
190.5	8,1 + 1,5 + 2,5
194	2,5
195.5	7,3 (lower plate)
199	2,5 + 8,1 + (7,3)
203.5	3,5
219.5	4,5 (lower plate)

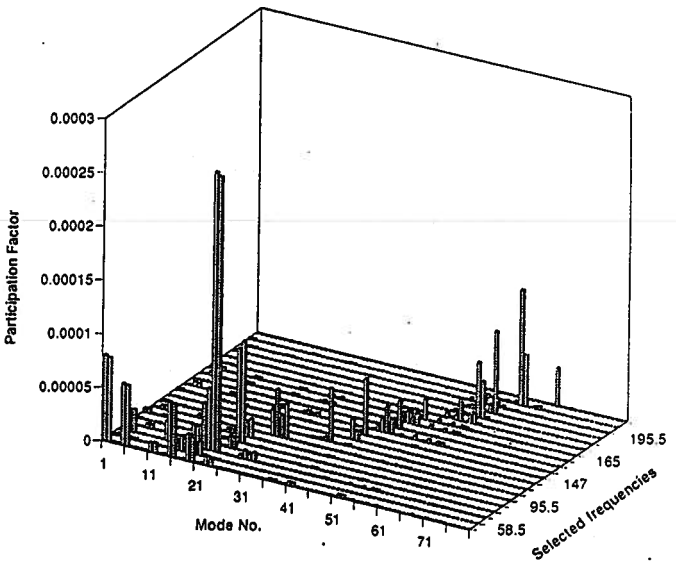

Fig.12. Participation factors for selected frequencies

5. COMPARISON AND DISCUSSION OF RESULTS

The comparison of the most relevant results, obtained from the different methods, can be performed by pairing the modal frequencies associated with identical mode numbers in Tables 1, 2 and 4. This analysis reveals that the agreement between the analytically and numerically calculated frequencies is quite satisfactory. The measured modal frequencies lie somewhat higher, but the average deviation of the measured resonance frequencies from their identifiable counterpart is certainly less than 5 Hz. (It has been revealed by carrying out careful stepped sine measurements that some of the variation of the measured modal frequencies were caused by temperature changes during the measurement series.)

The correspondence of the mode shapes is less convincing but perhaps still satisfactory to support the presented theory. The analytically calculated mode shapes are quite similar to the measured ones for certain frequencies (see e.g. for the 94 Hz mode in Figs. 3a, 4a and 7.) However, considerable deviations were also found in several cases. Reminding that our numerical calculations resulted in forced responses rather than freely vibrating modes, less agreement might we anticipate in advance.

Another important difference between the calculated and measured results is that many of the lateral modes and some of the longitudinal ones, especially those expected in the cavity, cannot be identified in the experiments and some of them do not appear in the numerical results either. This is thought to be caused by the too symmetric positioning of the loudspeaker inside the excitation enclosure, caused by spatial constraints.

Finally, it is worth to compare the results of our detailed investigations with those of the classical acoustic models, discussed in point 2.1. The calculated mass-air-mass natural frequency of our system lies around 98.5 Hz. As one can see is Fig.4. and in Table 2, we have three important modes in this region , out of which the acoustic radiation at 102 Hz is one of the strongest. This agreement is rather paradoxical, bearing in mind that the behaviour of the structural elements of our system is far from that of a concentrated mass.

6. CONCLUSIONS

1. The vibro-acoustical behaviour of a finite double wall system in the low frequency range can be successfully investigated by the methods presented. The natural frequencies of the coupled structural-acoustical system could be predicted with an accuracy of less than 5Hz and the obtained mode shapes show satisfactory agreement as well.

2. The coupling in the investigated system is highly "asymmetric": the structural response is much less influenced by the presence of the cavity, than the cavity's response is by the enclosing plates. This is in contrast with earlier achievements for shallow cavities backed by one flexible plate only.

3. The applied coupled FE-BE method is capable to handle the coupling mechanisms in double-wall structures.

4. The calculation of the mass-air-mass resonance frequency of a double-wall structure on the basis of a simple two dof acoustic system results in reasonable estimation of an important mode, but incapable of predicting the response of the system around this frequency.

7. REFERENCES

1. Beranek, L.L. and Work, G.A.: "Sound transmission through multiple structures containing flexible blankets"
   J. Acoust. Soc. Amer., 1949, Vol.21, 419-428.p.
2. London, A.: "Transmission of reverberant sound through double walls"
   J. Acoust. Soc. Amer., 1950, Vol.22, 270-279.p.
3. Cremer, L. and Heckl, M.: "Körperschall"
   Springer-Verlag, Berlin, 1967
4. Fahy, F.J.: "Sound and structural vibration. Radiation, transmission and response"
   Academic Press, London, 1985
5. Mulholland, K.A. - Parbrook,H.D. and Cummings,A.: "The transmission loss of double panels"
   J. Sound Vib., 1967, Vol.6, No.3, 324-334.p.
6. Trochidis, A. and Kalaroutis, A.: "Sound transmission through double partitions with cavity absorption"
   J. Sound Vib., 1986, Vol.107, No. 2., 321-327.p.
7. Lauriks, W., Mees, P. and Allard, J.F.: "The acoustic transmission through layered systems"
   J. Sound Vib., 1992, Vol.155, No.1., 125-132.p.
8. Dowell, E.H., Gorman III, G.F. and Smith, D.A.: "Acoustoelasticity: General theory, acoustic natural modes and forced response to sinusoidal excitation, including comparisons with experiment"
   J. Sound Vib., 1977, Vol.52, No.4, 519-542.p.
9. Pan,J. and Bies, D.A.: "The effect of fluid-structural coupling on sound waves in an enclosure - Theoretical part"
   J. Acoust. Soc. Amer., 1990, Vol. 87, No. 2, 691-707.p.
10. Sas,P., Van de Peer,J. and Augusztinovicz, F.: "Development of an analysis procedure for the assess ment of insertion loss characteristics of double wall structures"
    Proc. 9th Int. FASE Symposium on New Measurement Methods in Acoustics, Balatonfüred, 1991, 196-199.p.
11. Sas, P., Bao, C., Augusztinovicz, F. and Van de Peer, J.: "Active control of sound transmission through a light-weight double-panel partition"
    Proc. of the 17th Int. Sem. on Modal Analysis, Leuven, 1992, Part II. 743-764.p.
12. Sas, P., Van de Peer, J. and Augusztinovicz, F: "Modelling the vibro-acoustic behaviour of a double wall structure"
    DGLR/AIAA Paper #92-02-095, Proc. of the 14th Aeroacoustics Conference, Aachen, 1992, Vol.II., 561-570.p.